Applied Clay Science 88–89 (2014) 33–38

Contents lists available at ScienceDirect

Applied Clay Science

journal homepage: www.elsevier.com/locate/clay

Research paper

Montmorillonite as a multifunctional adsorbent can simultaneously remove crystal violet, cetyltrimethylammonium, and 2-naphthol from water

Runliang Zhu [a,b,*], Qingze Chen [a], Hanyang Liu [b], Fei Ge [b], Lifang Zhu [c], Jianxi Zhu [a], Hongping He [a]

[a] Guangzhou Institute of Geochemistry, Chinese Academy of Sciences, 510640, China
[b] Environmental Science and Technology Department, Xiangtan University, 411105, China
[c] Zhejiang Water Conservancy and Hydropower College, Hangzhou 310018, China

ARTICLE INFO

Article history:
Received 18 May 2012
Received in revised form 11 December 2013
Accepted 13 December 2013
Available online 7 January 2014

Keywords:
Montmorillonite
Adsorption
Wastewater treatment
Organic contaminants

ABSTRACT

The adsorptive behaviors of crystal violet (CV), cetyltrimethylammonium (CTMA), and 2-naphthol to montmorillonite (Mt) using a simultaneous-adsorption process were studied in this work. The adsorption results showed that under the experimental concentrations both CV and CTMA were almost completely removed by Mt. XRD and FTIR characterization results showed that the adsorbed CV and CTMA formed CTMA–CV aggregates within the interlayer spaces of Mt, and these aggregates served as accommodation spaces for the adsorption of 2-naphthol. The adsorption isotherms of 2-naphthol fitted linear equation well in the simultaneous-adsorption process, suggesting that partition should be the dominant mechanism for uptaking 2-naphthol. Combining the fact that CV alone formed aggregates showed nonlinear adsorption isotherms and much weaker adsorption capacity towards 2-naphtol than CTMA alone formed aggregates, one would expect that CTMA played a dominant role in the adsorption of 2-naphthol to CTMA–CV aggregates. In addition, the CTMA–CV aggregates have better adsorption capacity towards 2-naphthol than the combination of CTMA aggregates and CV aggregates do. FTIR results showed that CV could adjust the arrangement of CTMA in the CTMA–CV aggregates, which might be the reason for the enhanced adsorption capacity. Results of this work suggest that montmorillonite can be used as a low-cost and high-efficient adsorbent for the simultaneous removal of different types of organic contaminants from water.

1. Introduction

Montmorillonite (Mt) is a 2:1 type clay mineral composed of one octahedral sheet sandwiched by two tetrahedral sheets. Due to isomorphous substitution effect, Mt layers contain negative charges, which are counterbalanced by inorganic cations (e.g., Na^+, Ca^{2+}) (Brigatti et al., 2006). These inorganic cations are exchangeable, making Mt efficient adsorbent for various cationic contaminants, such as heavy metals (Bailey et al., 1999; Bhattacharyya and Gupta, 2008; Krishna and Susmita, 2006), cationic dyes (Eren and Afsin, 2008; Gupta and Suhas, 2009; Rytwo and Ruiz-Hitzky, 2003), and cationic surfactants (Li and Rosen, 2000; Li et al., 2006; Ma and Zhu, 2007). After the adsorption of organic cations, interlayer space of Mt can change from hydrophilic to hydrophobic, and the resulting materials, also known as organoclays, have been used as efficient adsorbents for hydrophobic organic contaminants (HOC) (Chen et al., 2005; Ramesh et al., 2007; Rytwo and Gonen, 2006; Shen, 2002, 2004; Zhu et al., 2007). Therefore, Mt can simultaneously remove both organic cations and HOC from wastewater, and it has been considered as a low-cost and high-efficient adsorbent for wastewater containing different organic contaminants (Ma and Zhu, 2007; Özcan et al., 2005; Rytwo and Gonen, 2006; Wei et al., 2009; Zhu and Ma, 2008).

Since Mt generally shows high affinity towards organic cations, the removal efficiency of HOC by Mt has drawn much more attention in the simultaneous-adsorption process (i.e., one-step-adsorption process). Several previous studies showed that the adsorptive behavior of HOC on Mt in this adsorption process strongly depends on the structure of intercalated organic cation (Ma and Zhu, 2007; Shen, 2002; Wei et al., 2009), similar to the adsorptive behavior of traditional organoclay, previously synthesized before the adsorption of HOC. For example, Wei et al. (2009) reported that in the simultaneous-adsorption process 2-naphthol was adsorbed on crystal violet (CV) intercalated Mt by a surface adsorption mechanism; while Ma and Zhu (2007) proposed that phenol was partitioned into the pseudo-organophase formed by cetyltrimethylammonium (CTMA) aggregates.

Numerous studies have shown that the arrangement of the intercalated cations can evidently influence the capacity of organoclays for adsorbing HOC (Chen et al., 2005; Churchman et al., 2006; Zhu et al., 2007, 2010). For the organoclays synthesized with small, compact organic cations (e.g., tetramethylammonium, TMA), increasing the

* Corresponding author at: Guangzhou Institute of Geochemistry, Chinese Academy of Sciences, 510640, China. Tel./fax: +86 20 85297603.
E-mail address: zhurl@gig.ac.cn (R. Zhu).

0169-1317/$ – see front matter © 2013 Elsevier B.V. All rights reserved.
http://dx.doi.org/10.1016/j.clay.2013.12.010

intermolecular distance of the intercalated cations will lead to larger exposed siloxane surface areas (main adsorption sites for HOC), which then can increase the adsorption capacity of this type of organoclays (Ruan et al., 2008; Shen, 2004). With respect to the organoclays synthesized with large, flexible organic cations (containing at least one long alkyl chains, e.g., CTMA), adjusting the arrangement of alkyl chain aggregates within the interlayer space of organoclays may also enhance their adsorption capacity (Zhu et al., 2007, 2010). According to these findings, several methods have been developed to improve the adsorption capacity of the organoclays. For example, reduced-charge Mt has been used to synthesize TMA-Mt, and the resulting organoclays will have larger surface areas and better adsorption capacity (Ruan et al., 2008). Cationic polymers (e.g., polyacrylamide) have been employed to simultaneously intercalate Mt with CTMA. Due to the high charge/volume ratio of the cationic polymers, the arrangement of CTMA can be adjusted, and the resulting organoclays show better adsorption capacity towards HOC (Zhu et al., 2010). As such, in the simultaneous-adsorption process the adsorptive behaviors of HOC may also be influenced by the arrangement of the intercalated organic cations, especially when wastewater contains different types of organic cations, since the co-existing organic cations may influence each other's arrangement within the interlay space of Mt. However, the related researches have not been well concerned yet until now.

The objectives of this work are (1) to investigate how the arrangement of cationic dyes and cationic surfactants can be influenced by each other within the interlayer spaces of Mt, and (2) to examine the adsorptive behaviors of the resulting organoclays towards HOC in the simultaneous-adsorption process. CV, CTMA, and 2-naphthol were selected as representatives of cationic dye, cationic surfactant and HOC, respectively. Results of this work may provide new information for understanding the adsorptive behaviors of organoclays and for the application of Mt in the treatment of wastewater containing multiple organic contaminants.

2. Materials and methods

2.1. Materials

The raw Mt sample (purity > 95%) with the structural formula of $Na_{0.016}$ $K_{0.020}Ca_{0.392}[Al_{2.518}Fe_{0.450}$ $Mg_{1.104}Ti_{0.360}Mn_{0.004}][Si_{7.910}Al_{0.090}]$ $O_{20}(OH)_4 \cdot nH_2O$, was obtained from Inner-Mongolia, China (Zhu et al., 2007, 2010). The net charge of the clay mineral was −0.82 *e* per unit cell, and its cation exchange capacity (CEC) was 108 cmol/kg. Cetyltrimethylammonium bromide, CV, and 2-naphthol of analytical grade were supplied by Shanghai Chemical Co. (China). All of the reagents were used as received.

2.2. Adsorption experiment

For comparison, the following batch adsorption experiments were carried out: (1) simultaneous adsorption of CV and 2-naphthol to Mt; (2) simultaneous adsorption of CTMA and 2-naphthol to Mt; and (3) simultaneous adsorption of CV, CTMA, and 2-naphthol to Mt. The obtained organoclays in above three adsorption systems were denoted as CV–Mt, CA–Mt, and CA–CV–Mt, respectively. The added amount of CV was controlled at 0.2 or 0.4 times CEC of Mt, and the added amount of CTMA was controlled at 0.2, 0.4, or 0.6 times CEC of Mt. The initial concentrations of 2-naphthol ranged from 5 to 200 mg/L. During the adsorption processes, 0.2 g Mt was combined with 20 mL solution (containing desired amount of above chemicals) in 25 mL glass centrifuge tubes. Then the tubes were sealed with Teflon-lined caps and shaken for 8 h at 25 °C. Preliminary experiments showed that the adsorption equilibrium was reached within 8 h. After centrifugation at 2000 *g* for 30 min, the concentration of 2-naphthol in supernate was detected using a UV–vis spectrophotometer at the wavelength of 224 nm. Control experiments showed that in the tested concentration range, both CV and CTMA could be almost completely adsorbed by Mt (over 99.5%), and the remaining CV and CTMA did not have evident influence on the detection of 2-naphthol.

2.3. X-ray diffraction and FTIR characterization

The X-ray diffraction (XRD) patterns of the Mt samples were recorded using a Bruker D8 ADVANCE X-ray diffractometer, operating at 40 kV and 40 mA with Cu Kα radiation. After the equilibrium adsorption of CV and/or CTMA, the resulting organoclays were separated from the water by 2 min centrifugation at 2000 *g*. Then the separated organoclay pastes were pressed on sample support and followed immediately by XRD measurement. The patterns were recorded for a 2θ range between 1° and 20° at a scanning speed of 2°/min. After that, the organoclays samples were dried at 60 °C for 12 h and then ground to pass 100 mesh sieves. The dry powders were then pressed on the sample support for further XRD measurement. Basal spacings were determined from the 2θ values of the corresponding basal reflections.

FTIR characterization for the dry samples was carried out on a Brucker Vertex-70 FTIR spectrophotometer. The spectra over the range of 4000–400 cm^{-1} were recorded with a resolution of 1.0 cm^{-1}. Proper amount of sample was mixed with KBr and milled to fine powder using a mortar and pestle. The powder was then made into a fragile pellet using a compression machine, and then the pellet was placed inside a supporting cell for infrared analysis. Sixty four interferograms were collected for each sample.

3. Results and discussion

3.1. Characterization results

XRD has been proved as a powerful tool in characterizing the structure of organoclays. The potential arrangements of intercalated organic cations were proposed according to the obtained basal spacing of organoclays and the size of organic cations (He et al., 2006; Xi et al., 2005). In this work, the XRD patterns of both dry and water saturated organoclays were obtained (Fig. 1), and accordingly the basal spacings were calculated (Table 1S). According to previous studies (He et al., 2006; Xi et al., 2005), CTMA should first adopt lateral-monolayer arrangement and then lateral-bilayer arrangement within the interlayer space of dry CA–Mt, as its loading level increased from 0.2 CEC to 0.6 CEC. Water saturated CA–Mt has larger basal spacing than the corresponding dry CA–Mt and the wet Mt, consistent with previous studies (Zhu et al., 2011), indicating the incorporation of large amount of water molecules to the interlayer space of the wet samples.

The basal spacing of dry CV–0.2Mt is 1.46 nm, which means that the gallery height is only 0.5 nm, suggesting flat arrangement of CV within the interlayer space of 0.2CV–Mt. After water saturation, the basal spacing of CV–0.2Mt increased to 1.99 nm. Double peaks corresponding to the basal spacings of 1.46 nm and 1.87 nm are shown for dry 0.4CV–Mt. For the wet 0.4CV–Mt, however, it has only one diffraction peak at 2.11 nm. These results also suggest that large amount of water molecules have entered into the interlayer space of wet CV–Mt.

The basal spacings of dry CA–CV–Mt are much larger than those of dry CA–Mt and dry CV–Mt, and they are generally proportional to the loaded amount of CTMA and CV, indicating the simultaneous intercalation of CTMA and CV into the interlayer spaces of CA–CV–Mt. After water saturation, the basal spacings of CA–CV–Mt can be further expanded. However, the expansion is quite small (no more than 0.1 nm) for most of the CA–CV–Mt, except for 0.4CA–0.2CV–Mt and 0.6CA–0.2CV–Mt, the two samples with lower CV but higher CTMA loading levels. In addition, although CA–0.4CV–Mt have large basal spacings in dry state than CA–0.2CV–Mt, the former series showed smaller basal spacing after water saturation. Combing with the fact that CA–Mt (with relatively high CTMA loading) swell more significantly than CV–Mt and CA–CV–Mt after water saturation, one can tell that

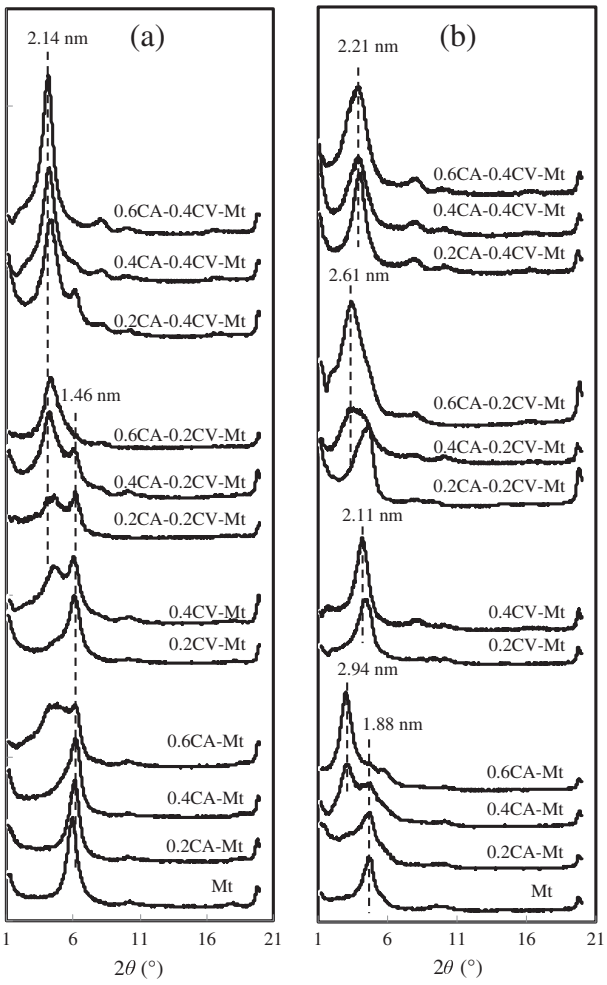

Fig. 1. The XRD patterns of the (modified) Mt. The results of both dry samples (a) and wet samples (b) were presented.

CTMA contributes to the expansion of CA–CV–Mt in the water while CV tends to hinder the expansion. The above results further proved that CTMA and CV simultaneously intercalated into the interlayer space of CA–CV–Mt, and then both can affect the expansion of CA–CV–Mt.

XRD patterns also show that some of the dry organoclays (e.g., 0.4CV–Mt) contain double diffraction peaks (Fig. 1a), suggesting heterogeneous layered structure for the corresponding samples. Similar results have been reported in previous publications for the intercalated Mt (He et al., 2006; Xi et al., 2005; Zhu et al., 2007). Interestingly, one of the diffraction peak for those samples appears at the same position as that of Mt. One possible explanation is that some of the interlayers of the organoclays are not intercalated by the organic cations. However, it could also be that the intercalated amount of organic cations is too small and cannot cause the expansion of the interlayers. Since most of the wet samples (except for 0.2CA–Mt and 0.4CA–Mt) have only one diffraction peak and the corresponding basal spacings are larger than that of wet Mt (Fig. 1b), one can propose that most of the interlayer spaces should have been intercalated by organic cations (otherwise these samples will still contain the diffraction peak of wet Mt).

Numerous studies have shown that these modes are extremely sensitive to the conformation of CTMA. The spectral region within 2700–3100 cm^{-1} shows the CH_2 asymmetric stretching mode ($\nu_{as}(CH_2)$) and symmetric stretching mode ($\nu_s(CH_2)$) of CTMA (Fig. 2a). With increasing CTMA loading level on CA–Mt, both $\nu_s(CH_2)$ and $\nu_{as}(CH_2)$ gradually shift towards low wavenumber (Table 2S), indicating the increase of ordering and packing density of CTMA, in agreement with previous studies (He et al., 2004). Interestingly, for the samples with lower CTMA loading levels (i.e., 0.2 and 0.4 CEC), both $\nu_{as}(CH_2)$ and $\nu_s(CH_2)$ have lower wavenumber for CA–CV–Mt than for CA–Mt, indicating that CV can increase the ordering and packing density of CTMA in low CTMA loading region. In addition, this effect seems to be more evident for the samples with more CV intercalation (0.4 CEC vs. 0.2 CEC). This further proves the simultaneous intercalation of CTMA and CV into the interlayer spaces of Mt. However, as CTMA loading level increased to 0.6 CEC, both $\nu_{as}(CH_2)$ and $\nu_s(CH_2)$ have similar wavenumber for the samples with or without CV, indicating that CV has little effect on the conformation of CTMA at this high CTMA loading level.

The spectral region within 800–1800 cm^{-1} shows the absorption band of aromatic C═C stretching vibration (1586 cm^{-1}), N-phenyl stretching vibration (1363 cm^{-1}), and N-CH_3 stretching vibration (1171 cm^{-1}) for solid CV (Fig. 2b). On the two CV–Mt samples, all the absorption bands of CV have much higher wavenumber (Table 2S), suggesting strong interaction between CV and Mt. In addition, on the CA–CV–Mt, the absorption band of both C═C stretching vibration and N-phenyl stretching vibration further shifted to higher wavenumber, indicating the obvious interactions between CV and CA. As such, the FTIR characterization results further prove the mutual influence on the arrangement of CA and CV within the interlayer space of CA–CV–Mt.

According to the above results the potential interlayer structures of water saturated CA–CV–Mt are presented in (Fig. 3). CTMA and CV associate with each other and form relatively large organic aggregates within the interlayer space, which can serve as adsorption medium for HOC. Water molecules are shown to locate near the inorganic cation and the siloxane surface to hydrate them. However, one should note that the microstructure presented in this paper is highly schematic. Since the interlayer space of CA–CV–Mt may simultaneously contain CTMA, CV, inorganic cations and water, their microstructure can be really complex and investigations are needed to further clarify it.

3.2. Adsorption of 2-naphthol on organoclays

The adsorption isotherms of 2-naphthol on CV–Mt and CA–Mt are compared in this paper (Fig. 4). Preliminary adsorption experiments showed that Mt can hardly uptake 2-naphthol. Therefore, the intercalated organic cations can significantly increase the affinity of the resulting organoclays towards 2-naphthol, and their adsorption capacity is shown to be proportional to the intercalated amount of organic cations. Under the same saturated CEC level, CA–Mt have much better adsorption capacity towards 2-naphthol than CV–Mt do. In addition, the adsorption isotherms on CV–Mt are obviously nonlinear, while those on CA–Mt appear to be linear. The linear equation and Freundlich equation are used to fit these adsorption isotherms to CA–Mt and CV–Mt, respectively. The obtained R^2 values clearly show that these obtained equations can fit the adsorption isotherms well (Table 1). The adsorption coefficient of HOC (K_d), which is defined by the ratio of adsorbed concentration to the aqueous concentration, can directly show the adsorption efficiency of HOC on an adsorbent (Zhu et al., 2007). The K_d values of 2-naphthol on CA–Mt were calculated from the slope of the linear equation of the adsorption isotherms (Table 1).

The adsorption capacity of 2-naphthol to the two serials of CA–CV–Mt (CV loading level of 0.2 and 0.4CEC respectively) increases with CTMA loading amount (Fig. 4). One interesting phenomenon is that the adsorption isotherms are approximately linear, even for the sample with CTMA loading level smaller than CV (i.e., 0.2CA–0.4CV–Mt). The linear equation was applied to fit the adsorption isotherms on CA–CV–Mt, and the obtained R^2 values (Table 1) show that the linear equation can fit these isotherms well. This suggests that 2-naphthol is adsorbed to CA–CV–Mt primarily by a partition mechanism. The K_d values for 2-naphthol adsorption on CA–CV–Mt are calculated accordingly (Table 1), and the results show that CA–CV–Mt have much better adsorption capacity than the corresponding CA–Mt (i.e., with the same CTMA loading). In addition, the CA–CV–Mt with the same loading amount of CTMA but different amount of CV have quite similar K_d

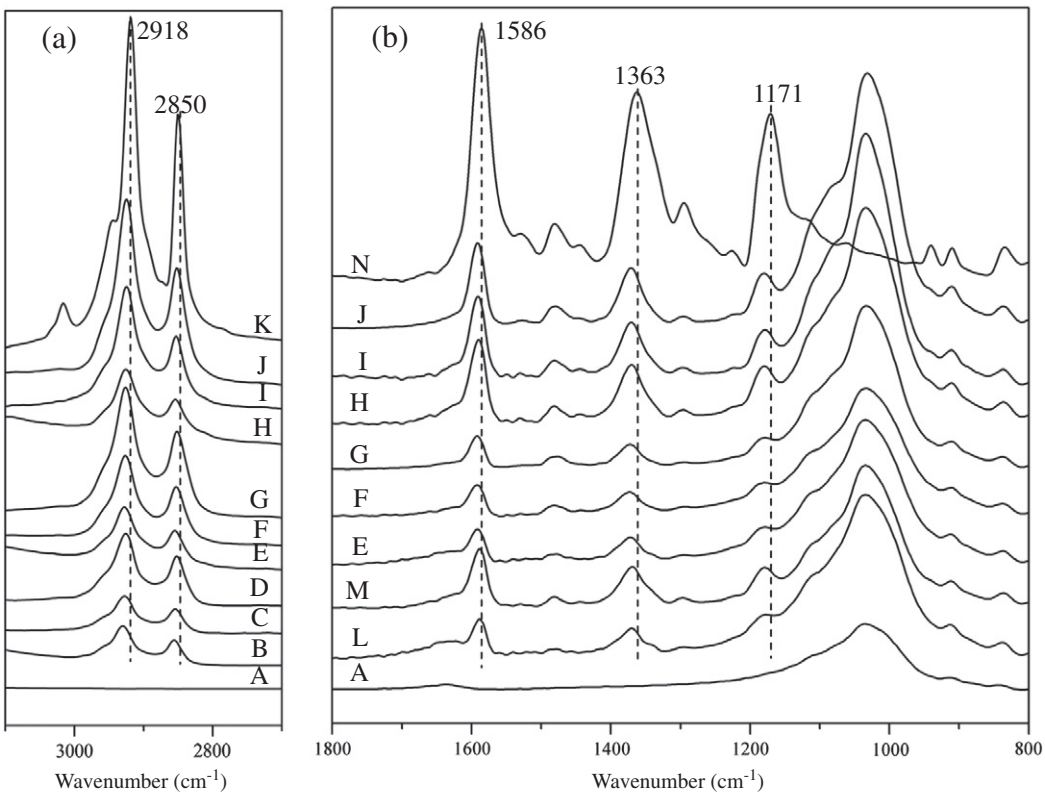

Fig. 2. The FTIR spectra of (modified) Mt. Spectra in the region 2700–3100 cm^{-1} (a) shows the absorption bands arising from CTMA, and in the region 800–1800 cm^{-1} (b) shows the absorption bands arising from CV. A: Mt; B: 0.2CA–Mt; C: 0.4CA–Mt; D: 0.6CA–Mt; E: 0.2CA–0.2CV–Mt; F: 0.4CA–0.2CV–Mt; G: 0.6CA–0.2CV–Mt; H: 0.2CA–0.4CV–Mt; I: 0.4CA–0.4CV–Mt; J: 0.6CA–0.4CV–Mt; K: CTMAB; L: 0.2CV–Mt; M: 0.4CV–Mt; N: CV.

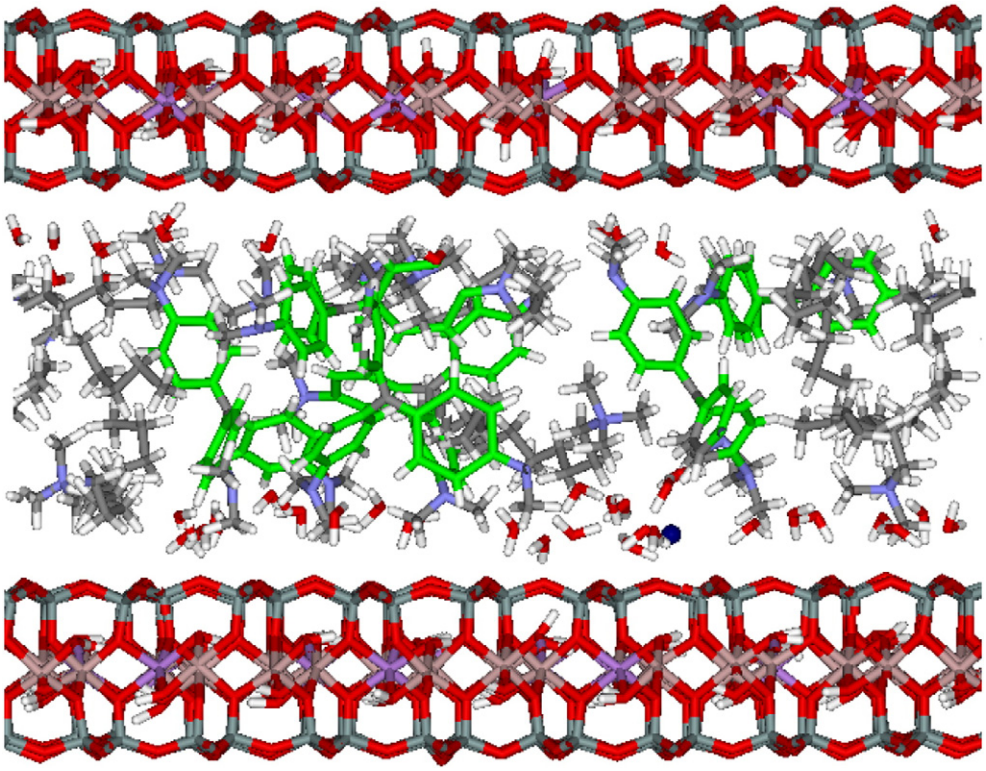

Fig. 3. Schematic drawing of the microstructure of water saturated CA–CV–Mt. Within the interlayer space of Mt, both CV (green line), CTMA (gray line) and water (red line) were shown.

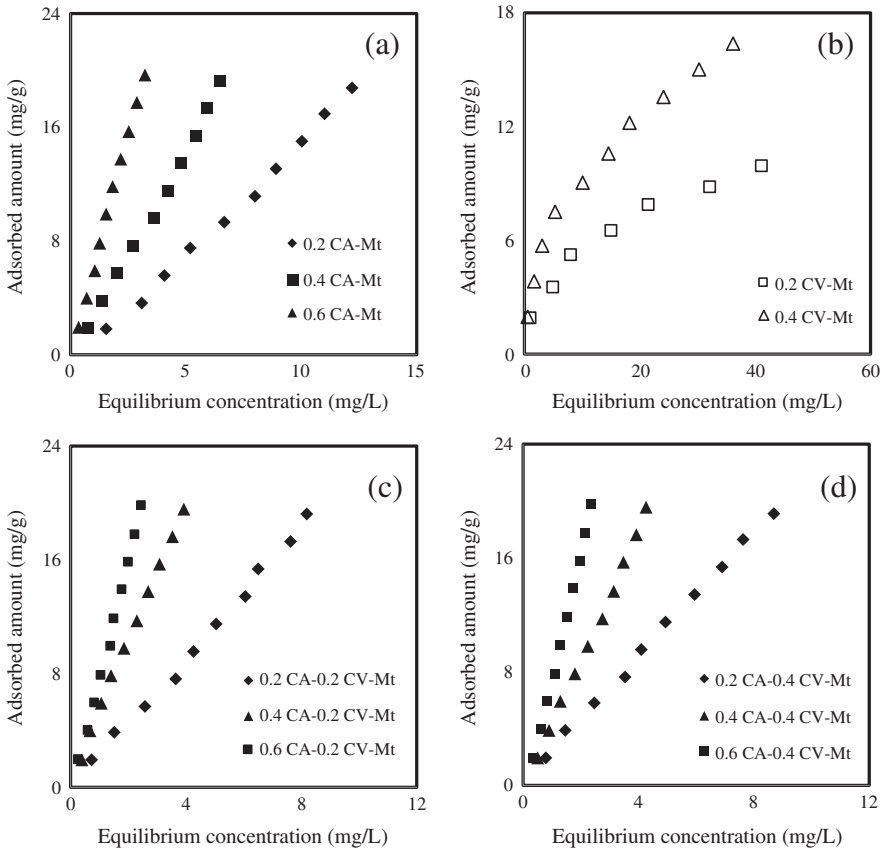

Fig. 4. Adsorption isotherms of 2-naphthol on various organoclays: (a) on CA–Mt, (b) on CV–Mt (c) on CA–CV–Mt with the same amount of CTMA, and (d) on CA–CV–Mt with the same amount of CV.

values, which suggests that CTMA should play a dominant role for the adsorption of 2-naphthol on CA–CV–Mt.

3.3. Potential mechanism for the enhanced adsorption of 2-naphthol to CA–CV–Mt

The above results once again proved that Mt can be a multifunctional adsorbent for the simultaneous removal of both organic cations and HOC from water. The adsorbed CV and CTMA can form hydrophobic aggregates within the interlayer space of Mt, and the resulting CA–CV–Mt will have better adsorption capacity than the CA–Mt and CV–Mt. The enhancement of adsorption capacity can be more evident by comparing the adsorption capacity of CA–CV–Mt with the combination of those of CA–Mt and CV–Mt (i.e., CA–Mt + CV–Mt). According to the obtained adsorption equations (Table 1), the adsorption isotherms of 2-naphthol to CA–Mt + CV–Mt can be calculated (Fig. 5). At relatively high 2-naphthol concentration range (>5 mg/L) 0.4CA–0.4CV–Mt has much better adsorption capacity than 0.4CA–Mt + 0.4CV–Mt. Similar results are observed for other serials of organoclays (Fig. 1S).

Generally, the enhancement of adsorption capacity of an adsorbent can be ascribed to two possible reasons: (1) the increase of adsorption sites on the adsorbent, and (2) the increase of interaction affinity for

Table 1
Linear or Freundlich regression results of 2-naphthol adsorption to organoclays. K_d is the adsorption coefficient obtained from the linear regression equation.

Organoclays	Regression equations	R^2	K_d (L/kg)
0.2CA–Mt	$y = 1.48x$	0.991	1480
0.4CA–Mt	$y = 2.98x$	0.996	2980
0.6CA–Mt	$y = 6.16x$	0.995	6160
0.2CV–Mt	$y = 1.87 \times^{0.45}$	0.991	–
0.4CV–Mt	$y = 3.07 \times^{0.46}$	0.987	–
0.2CA–0.2CV–Mt	$y = 2.29x$	0.996	2290
0.4CA–0.2CV–Mt	$y = 5.09x$	0.996	5090
0.6CA–0.2CV–Mt	$y = 7.76x$	0.992	7760
0.2CA–0.4CV–Mt	$y = 2.25x$	0.997	2250
0.4CA–0.4CV–Mt	$y = 4.45x$	0.997	4450
0.6CA–0.4CV–Mt	$y = 7.86x$	0.995	7860

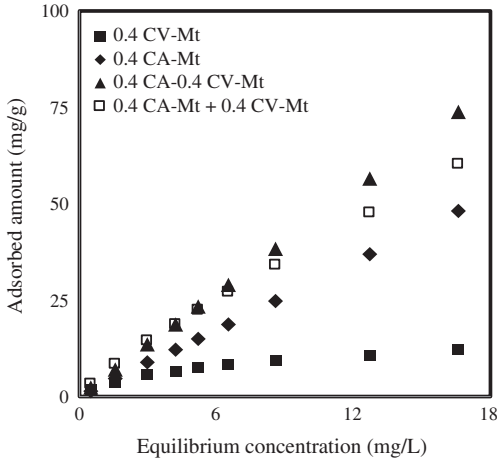

Fig. 5. Comparison of the adsorption capacity of 2-naphthol on 0.4CV–Mt, 0.4CA–Mt. and 0.4CA–0.4CV–Mt. 0.4CA–0.4CV-Mt had much better sorption capacity than 0.4CV–Mt and 0.4CA–Mt. At relatively high equilibrium concentration 0.4CA–0.4CV–Mt had better adsorption capacity than the combination of 0.4CV–Mt and 0.4CA–Mt (i.e., 0.4CV–Mt + 0.4CA–Mt).

the adsorbates. In the case of CA–CV–Mt, since CTMA and CV together can form larger hydrophobic aggregates (compared to the aggregates formed by CTMA or CV alone), one can expect that the accommodation volume for 2-naphthol will increase accordingly. On the other hand, it is also possible that the CTMA–CV aggregates have better affinity towards 2-naphthol. Previous studies showed that the arrangement of CTMA within CA–Mt can evidently influence the capacity of CA–Mt in adsorption of HOC, and CTMA aggregates with medium packing density have better adsorption capacity towards HOC (Zhu and Zhu, 2008; Zhu et al., 2007). As such, cationic polymer was employed to change the arrangement of CTMA, and the resulting organoclays were shown to have better affinity towards HOC (Zhu et al., 2010). Similar situation could happen to CA–CV–Mt as well, since in both cases CTMA seems to play a predominant role in the adsorption of HOC and CV can also change the arrangement of CA (e.g., enhancing its packing density).

Dye wastewater from textile industry always contains multiple organic contaminants and biodegradation treatment generally cannot effectively remove these contaminants. Although activated carbon can effectively adsorb most of these contaminants, its high price restricts its wide application. The results of this study showed that Mt, as a low cost adsorbent, can effectively remove all the three types of organic contaminants from water. In addition, the results also showed that the adsorbed cationic dye and cationic surfactant have mutual influence on their arrangement within the interlayer space of montmorillonite, which then leads to better adsorption capacity towards HOC. As such, montmorillonite has the potential to be widely used in dye wastewater treatment.

4. Conclusion

Mt can be used as a low-cost and high-efficient adsorbent to simultaneously remove CTMA, CV and 2-naphthol from wastewater. XRD and FTIR characterization results showed that the adsorbed CTMA and CV together will form hydrophobic CTMA–CV aggregates within the interlayer space of Mt, which then can evidently enhance the capacity of Mt in the adsorption of 2-naphthol. The linear adsorption isotherms suggest that 2-naphthol has been adsorbed primarily by partitioning into the CTMA–CV aggregates. In addition, the CTMA–CV aggregates show better adsorption capacity towards 2-naphthol than the combination of CTMA and CV alone formed aggregates. The enhanced adsorption capacity may be attributed to the larger volume of partition medium created by CTMA–CV aggregates. Meanwhile, results of this work also suggest that CV can change the arrangement of CTMA within CTMA–CV aggregates and then increase their interaction affinity towards 2-naphthol. This work proved that Mt can be used as multifunctional adsorbents for the simultaneous removal of different types of contaminants from wastewater.

Acknowledgment

This work was financially supported by the “One Hundred Talents program” of the Chinese Academy of Sciences (KZZD-EW-TZ-10), grants from the National Natural Science Foundation of China (41322014, 21177104), and Natural Science Foundation of Zhejiang province (Y5110238) were also acknowledged. This is Contribution No. IS-1796 from GIGCAS.

Appendix A. Supplementary data

Supplementary data to this article can be found online at http://dx.doi.org/10.1016/j.clay.2013.12.010.

References

Bailey, S.E., Olin, T.J., Bricka, R.M., Adrian, D., 1999. A review of potential low-cost sorbents for heavy metals. Water Res. 33, 2469–2479.
Bhattacharyya, K.G., Gupta, S.S., 2008. Adsorption of a few heavy metals on natural and modified kaolinite and montmorillonite: a review. Adv. Colloid Interf. Sci. 140, 114–131.
Brigatti, M.F., Galan, G.E., Theng, B.K.G., 2006. Structures and mineralogy of clay minerals. In: Bergaya, F., Theng, B.K.G., Lagaly, G. (Eds.), Handbook of Clay Science. Elsevier, Amsterdam, pp. 19–86.
Chen, B., Zhu, L., Zhu, J., 2005. Configurations of the bentonite-sorbed myristylpyridinium cation and their influences on the uptake of organic compounds. Environ. Sci. Technol. 39, 6093–6100.
Churchman, G.J., Gates, W.P., Theng, B.K.G., Yuan, G., 2006. Clays and clay minerals for pollution control. In: Bergaya, F., Theng, B.K.G., Lagaly, G. (Eds.), Handbook of Clay Science. Elsevier, Amsterdam, pp. 625–676.
Eren, E., Afsin, B., 2008. Investigation of a basic dye adsorption from aqueous solution onto raw and pre-treated bentonite surfaces. Dyes Pig. 76, 220–225.
Gupta, V.K., Suhas, 2009. Application of low-cost adsorbents for dye removal—a review. J. Environ. Manag. 90, 2313–2342.
He, H., Frost, R.L., Zhu, J., 2004. Infrared study of HDTMA$^+$ intercalated montmorillonite. J. Colloid Interface Sci. 60, 2853–2859.
He, H., Frost, R.L., Bostrom, T., Yuan, P., Duong, L., Yang, D., Xi, Y., Kloprogge, J.T., 2006. Changes in the morphology of organoclays with HDTMA$^+$ surfactant loading. Appl. Clay Sci. 31, 262–271.
Krishna, G.B., Susmita, S.G., 2006. Kaolinite, montmorillonite, and their modified derivatives as adsorbents for removal of Cu(II) from aqueous solution. Sep. Purif. Technol. 50, 388–397.
Li, F., Rosen, M.J., 2000. Adsorption of gemini and conventional cationic surfactants onto montmorillonite and the removal of some contaminants by the clay. J. Colloid Interface Sci. 224, 265–271.
Li, J., Zhu, L., Cai, W., 2006. Characteristics of organobentonite prepared by microwave as a sorbent to organic contaminants in water. Colloids Surf. A 281, 177–183.
Ma, J., Zhu, L., 2007. Removal of phenols from water accompanied with synthesis of organobentonite in one-step process. Chemosphere 68, 1883–1888.
Özcan, A.S., Erdem, B., Özcan, A., 2005. Adsorption of Acid Blue 193 from aqueous solutions onto BTMA-bentonite. Colloids Surf. A 266, 73–81.
Ramesh, A., Hasegawa, H., Maki, T., Ueda, K., 2007. Adsorption of inorganic and organic arsenic from aqueous solutions by polymeric Al/Fe modified montmorillonite. Sep. Purif. Technol. 56, 90–100.
Ruan, X., Zhu, L., Chen, B., 2008. Adsorptive characteristics of the siloxane surfaces of reduced-charge bentonites saturated with tetramethylammonium cation. Environ. Sci. Technol. 42, 7911–7917.
Rytwo, G., Gonen, Y., 2006. Very fast sorbent for organic dyes and contaminants. Colloid Polym. Sci. 284, 817–820.
Rytwo, G., Ruiz-Hitzky, E., 2003. Enthalpies of adsorption of methylene blue and crystal violet to montmorillonite —enthalpies of adsorption of dyes to montmorillonite. J. Therm. Anal. Calorim. 71, 751–759.
Shen, Y.H., 2002. Removal of phenol from water by adsorption flocculation using organobentonite. Water Res. 36, 1107–1114.
Shen, Y.H., 2004. Phenol sorption by organoclays having different charge characteristics. Colloids Surf. A 232, 143–149.
Wei, J., Zhu, R., Zhu, J., Ge, F., Yuan, P., He, H., Chen, M., 2009. Simultaneous sorption of crystal violet and 2-naphthol to bentonite with different CECs. J. Hazard. Mater. 166, 195–199.
Xi, Y., Frost, R.L., Kloprogge, T., Bostrom, T., 2005. Modification of Wyoming montmorillonite surface using a cationic surfactant. Langmuir 21, 8675–8680.
Zhu, L., Ma, J., 2008. Simultaneous removal of acid dye and cationic surfactant from water by bentonite in one-step process. Chem. Eng. J. 139, 503–509.
Zhu, R., Zhu, L., 2008. Thermodynamics of naphthalene sorption to organoclays: role of surfactant packing densities. J. Colloid Interface Sci. 322, 27–32.
Zhu, R., Zhu, L., Xu, L., 2007. Sorption characteristics of CTMA-bentonite complexes as controlled by surfactant packing density. Colloids Surf. A 294, 221–227.
Zhu, R., Wang, T., Zhu, J., Ge, F., Yuan, P., He, H., 2010. Structural and sorptive characteristics of the cetyltrimethylammonium and polyacrylamide modified bentonite. Chem. Eng. J. 160, 220–225.
Zhu, J., Wang, T., Zhu, R., Ge, F., Yuan, P., He, H., 2011. Expansion characteristics of organo montmorillonites during the intercalation, aging, drying and rehydration processes: effect of surfactant/CEC ratio. Colloids Surf. A 51, 317–322.